Evaluation of Finger Configuration for Partial Caging

Satoshi Makita[1] and Kazuyuki Nagata[2]

Abstract— **In caging, an object is geometrically confined by position-controlled robots and never escape from the constraint. Caging has some advantages over conventional grasping, and its applications have been performed not only in 2D but also in 3D scenes with various actual robots. However, the conditions of complete caging are not always satisfied due to limited robot configuration. This paper studies *partial caging*, in which an object is incompletely confined by robots or obstacles and is able to escape from the constraint. As an example of partial caging, a circular object moved in the planar hand is considered. We investigate an effect of arrangement of its fingertips, which prevents the object from escaping outside through the gap between the fingertips. Some simulation results show differences of difficulty of escaping for the object according to width of the gap and angle of the fingers. In addition, ease of entering the hand through the gap of the fingers is also evaluated. From these two scores on partial caging, we define an ability index for the hand, which represents the hand can easily capture an object and confine it without any finger motion.**

I. Introduction

This paper deals with a case of geometrical constraint based on caging and its arrangement of obstacles (or robots) to capture an object. We consider that a circular object is confined in a robot hand that surround almost the object (Fig. 1), and call this situation *partial caging*. Then the arrangement of the fingertip affects both ease of entering the robotic cage and difficulty of escaping from there, like a fish trap (Fig. 2). In this paper, a simplified scenario of partial caging in two-dimension is considered. The arrangement of the fingers can be utilized for planning of caging as preshaping of robot hands for grasping and also for formation of decentralized robots.

Caging is a method to constrain an object by robots geometrically, where the robots are located around the object to confine the cage region [1]. The caged object can be restricted to move only in the constricted region and cannot escape from the cage formed by the robots. Thus even position-controlled robots can constrain objects, and then it is an advantage over conventional grasping or fixturing, which usually need force control. The methods of caging has been proposed not only in 2D but also in 3D scenes. 2D caging are often achieved by multiple circular or pointed robots as [1], but 3D caging are not only by pointed robots [2] but also by a practical robot hands [3], [4].

For *complete caging* mentioned above, where an object is completely confined and never escape from the constraint, some mathematical sufficient conditions for caging must be satisfied by robots. However, it is often difficult for some limited robots for lack of number or mechanical restriction of multifingered hands.

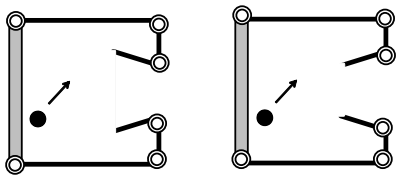

Fig. 1. Differences of difficulty of escaping according to the finger posture

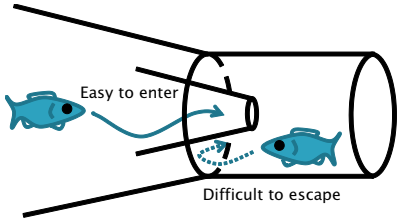

Fig. 2. Fish trap (A case of partial caging)

Here we consider *partial caging* [5], where an object is not completely confined by robots and obstacles. Nevertheless the object hardly escapes from the constraint if its paths to escape are narrow and/or limited. Thus partial caging can sometimes be substituted for *complete* caging, and it is an advantage especially for the limited robots mentioned above.

In this paper, we study on a simplified partial caging scenario, where an object is confined in the two-dimensional hand with a gap between its fingertips (Fig. 1), and investigate an effect of the angle of the fingertips for the object to pass through the gap. This situation can be regarded as a simplified robotic application inspired fish traps (Fig. 2). If efficient arrangements of surroundings to confine the objects are revealed, they can be applied to design and control strategies of robots for caging and/or enclosing. A robot hand like fish traps, for example, may easily capture an object but hardly release it, without any finger motion.

A. Related Works

The concept of caging is considered to be firstly proposed by Kuperberg [6] and has been studied as preshaping of grasping or fixturing by a gripper hand or multiple mobile robots in 2D plane independently: 2D caging as preshaping of a gripper that has two circular fingertips [1]; caging non-convex polytopes by two pointed fingers [2]; two-fingered-caging [7]; three or more fingertips [8], [9]; manipulation via caging by multiple robots [10]; derivation of caging

[1]S. Makita is with Dept. of Control Engineering, Sasebo College, National Institute of Technology, 1-1 Okishincho, Sasebo, Japan, makita@sasebo.ac.jp

[2]K. Nagata is with Vision and Manipulation Research Group, Intelligent Systems Institute, The National Institute of Advanced Industrial Science and Technology 1-1-1 Umezono, Tsukuba, Japan, k-nagata@aist.go.jp

conditions by distributed multiple robots and demonstration [11]. While a lot of works focus on caging in 2D scenes, the followings deal with caging in 3D scenes and actual robot hands: *caging grasps* by a manipulator and a humanoid robot in 3D scenes [3]; *caging-based grasping*, which rigid bodies inside the hand capture an object geometrically and soft parts covering the rigid bodies contact with the object [12]; derivation of sufficient conditions for caging of some primitive objects by a particular multifingered hand [4]: *grasping by caging*, where some fingers (poles) cage an object on the plate and grasp it by shrinking the caged region [13].

Other geometrical constraints derived from caging are recently studied. Jiang et al. proposed *gravity caging* to place an object on a particular location [14]. This idea uses caging or geometrical constraint partially and the gravitational force prevents the placed object from escaping toward unconfined direction. Makapunyo et al. studied quality of *partial cage*, in which an object is incompletely caged by robots, and then the object can escape from the caging formation in 2D scenes [5]. They tested ease of escaping from the robots formation for some objects by some path planners.

This paper also studies quality of *partial caging* in two-dimension in cases that a circular object can be partially surrounded by a robot hand (Fig. 1). In this case, there are some paths for the object to escape outside of the hand although they are sometimes narrow and difficult to pass through for the object such as traps for small animals (Fig. 2). On the other hand, the object can also enter the "partial cage" by itself through the gap of fingertips. As a consequence, the object is to be captured and constrained by the robot without any finger motion.

For more simplicity of the problem, let us consider the two-dimensional hand like a tray with walls in three dimension, which can be inclined by a manipulator with 2 degrees of freedom (DOF), as shown in Sec. II. We examine both ease of entering the hand (EoEn) and difficulty of escaping from the hand (DoEs) for a circular object, with changing parameters of the finger arrangement: width of the gap between fingertips and angle of the fingertip. First we describe the formulas about the settings of partial caging by the hand, physical phenomena about the caged object and motion of the manipulator controlling the hand. Next, we show some simulation results that changing the finger parameters affects to both *EoEn* and *DoEs* about the partially closed region.

II. Model of Partial Caging by a Robot Hand

A. Assumptions and Notations

We assume the following conditions for our simulation.

- Simulations are performed on two dimensional hand that is manipulated by a manipulator with 2 DOF.
- A single circular object moving in the hand without any slipping and any friction is observed. Then the center of the object is called as *moving point*.

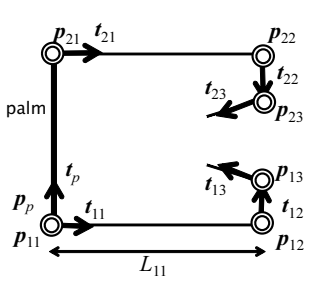

Fig. 3. Setting of the hand

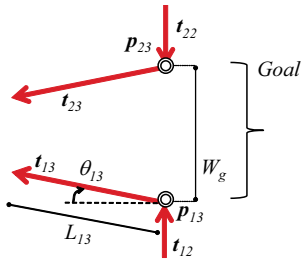

Fig. 4. Setting of the goal (fingertips)

- Fingers of the hand confine the moving object. Generally in this paper, *limbs* represent both the fingers and the palm of the hand.
- The hand forms a polygonal shape and has a gap between the fingertips as a *goal*, from which the moving object can enter the hand from outside and also escape from the hand (Fig. 1). The fingertips behave like a double door that is opened and closed with changing their joint angles.
- Only gravitational force is applied to the object.
- Every volume of the joints is negligible small.

We define the following notations.

- $\boldsymbol{p}_p \in \mathbb{R}^2$: the position of the moving point.
- $\boldsymbol{v}_p \in \mathbb{R}^2$: the velocity of the moving point.
- $\boldsymbol{p}_i \in \mathbb{R}^2$: the position of the joint of the i-th limb.
- $\boldsymbol{t}_i \in \mathbb{R}^2$: the unit direction vector along the i-th limb.
- $\boldsymbol{n}_i \in \mathbb{R}^2 := \begin{bmatrix} \cos\frac{\pi}{2} & -\sin\frac{\pi}{2} \\ \sin\frac{\pi}{2} & \cos\frac{\pi}{2} \end{bmatrix} \boldsymbol{t}_i$: the unit normal vector of the i-th limb.
- $L_i \in \mathbb{R}^1$: the length of the i-th limb.
- $M_o \in \mathbb{R}^1$: the mass of the moving object.
- $r_o \in \mathbb{R}^1$: the radius of the moving object.

As the assumptions, the hand confining the moving object has an gap between both fingertips as a goal, through which the object can pass. Thus fingertips behave as a gate at the front of the goal. The limbs of the hand are numbered as Fig. 3 ($i = p, 11, \ldots 21, \ldots$).

The parameters about the goal and the gate are below (Fig. 4):

- L_g: the length of each fingertip. and then $L_{13} = L_{23} = L_g$.
- $W_g := \|\boldsymbol{p}_{13} - \boldsymbol{p}_{23}\|$: the width of the goal that defined as the width of the gap between the fingertips.
- $\theta_g := \theta_{13} = -\theta_{23}$: the angle of the gate that defined as the joint angle of every fingertip.

For the simplicity of explanation, we define $\theta_g = 0$ when the fingertip is perpendicular to the linked limbs. Hence the gate is closing while $\theta_g > 0$ and vice versa.

B. Equation of the Moving Object's Motion

The circular object in the hand moves without any slipping in two-dimensional space, and the center of the object are called as *moving point*. For randomized movement of the hand, it is manipulated and inclined by a manipulator with 2 DOF like a universal joint (Fig. 5). When joint variables

of the manipulator are defined as: θ_{j1} and θ_{j2}, the relative rotation matrix between the frame of the hand and the reference frame defined at 1st joint of the manipulator, ${}^{O}_{P}\boldsymbol{R}$, is written as follows:

$$
\begin{aligned}
{}^{O}_{P}\boldsymbol{R} &= \begin{bmatrix} \cos\theta_{j1} & 0 & \sin\theta_{j1} \\ 0 & 1 & 0 \\ -\sin\theta_{j1} & 0 & \cos\theta_{j1} \end{bmatrix} \begin{bmatrix} 1 & 0 & 0 \\ 0 & \cos\theta_{j2} & -\sin\theta_{j2} \\ 0 & \sin\theta_{j2} & \cos\theta_{j2} \end{bmatrix} \\
&= \begin{bmatrix} \cos\theta_{j1} & \sin\theta_{j1}\sin\theta_{j2} & \sin\theta_{j1}\cos\theta_{j2} \\ 0 & \cos\theta_{j2} & -\sin\theta_{j2} \\ -\sin\theta_{j1} & \cos\theta_{j1}\sin\theta_{j2} & \cos\theta_{j1}\cos\theta_{j2} \end{bmatrix}, \qquad (1)
\end{aligned}
$$

where θ_{j1} rotates around $Y-$axis of the reference frame and θ_{j2} rotates around $X-$axis of the next frame. Thus the gravitational acceleration on the hand, $\boldsymbol{g}_P \in \mathbb{R}^3$, can be calculated with that on the reference frame, $\boldsymbol{g}_O := [0, 0, -g]^T \in \mathbb{R}^3$, as,

$$
\begin{aligned}
\boldsymbol{g}_P(\theta_{j1}, \theta_{j2}) &= {}^{O}_{P}\boldsymbol{R}^{-1}\boldsymbol{g}_O \\
&= \begin{bmatrix} g\sin\theta_{j1} & -g\cos\theta_{j1}\sin\theta_{j2} & -g\cos\theta_{j1}\cos\theta_{j2} \end{bmatrix}^T. \qquad (2)
\end{aligned}
$$

In two dimensional space, only the first and second components of the vector, $\boldsymbol{g}_P$, are used and the third is not considered. Thus (2) is rewritten as follows:

$$
\boldsymbol{g}_P(\theta_{j1}, \theta_{j2}) = \begin{bmatrix} g\sin\theta_{j1} & -g\cos\theta_{j1}\sin\theta_{j2} \end{bmatrix}^T \in \mathbb{R}^2. \qquad (3)
$$

With the gravitational acceleration (3), the equation of the moving point's motion can be expressed as:

$$
M_o\ddot{\boldsymbol{p}}_p = M_o\boldsymbol{g}_P(\theta_{j1}, \theta_{j2}). \qquad (4)
$$

C. Rebound Between the Moving Object and the Fingers

When the moving point reaches the distance of r_o from a limb, the moving object makes contact with the limb. Thus we can examine the collisions between the moving object and the walls, with the following inequalities:

$$
\boldsymbol{v}_p \cdot \boldsymbol{n}_i < 0, \qquad (5)
$$

$$
0 \le \left(\boldsymbol{p}_p - \boldsymbol{p}_i\right) \cdot \boldsymbol{n}_i \le r_o, \qquad (6)
$$

$$
0 \le \left(\boldsymbol{p}_p - \boldsymbol{p}_i\right) \cdot \boldsymbol{t}_i \le L_i. \qquad (7)
$$

In regard to collisions with the gate (the fingertip), however, the moving object can have contact with both sides and the end of it. Thus we have to set an additional normal vector on the opposite side of the gate for calculations. When the object have collision with the end point of the gate (the fingertip), the unit normal vector of the end point, $\boldsymbol{n}_{e,i}$ is calculated with as,

$$
\boldsymbol{n}_{e,i} = \frac{\boldsymbol{p}_p - \boldsymbol{p}_{e,i}}{\|\boldsymbol{p}_p - \boldsymbol{p}_{e,i}\|}, \qquad (8)
$$

where $\boldsymbol{p}_{e,i}$ is the position vector of the end point. And then, the object has collision with the end point when two following equations are satisfied.

$$
\|\boldsymbol{p}_p - \boldsymbol{p}_{e,i}\| \le r_o \qquad (9)
$$

$$
\boldsymbol{t}_{e,i} \cdot \boldsymbol{n}_{e,i} > 0, \qquad (10)
$$

where $\boldsymbol{t}_{e,i}$ is a unit direction vector that goes along the gate. Similarly when the object may have collision with a joint, the collision test mentioned above is examined.

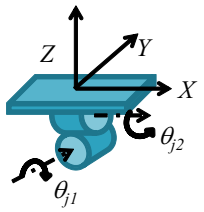

Fig. 5. A two DOF manipulator inclining the hand

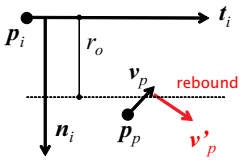

Fig. 6. A rebound of the moving point

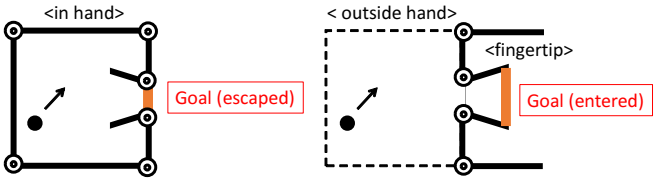

Fig. 7. Goal judgment for simulations

Changed velocity of the moving point after rebound, $\boldsymbol{v}'_p$ (Fig. 6) can be written as:

$$
\boldsymbol{v}'_p = \boldsymbol{v}_p - (1 + e_r)(\boldsymbol{v}_p \cdot \boldsymbol{n}_i)\boldsymbol{n}_i, \qquad (11)
$$

where e_r is the coefficient of restitution between the moving object and every limb.

III. Evaluation of Partial Caging Quality

In this paper, we investigate an effect of the finger arrangement to ease of entering the hand (EoEn) and difficulty of escaping from the hand (DoEs) for the moving object, with changing the width of the gap between fingertips (the goal), the angle of the fingertips (the gate) and the size of the object. The two dimensional hand is manipulated and declined by a two DOF manipulator. The object confined in the hand is circular and moves according to the gravitational acceleration on the planar hand without any slipping. After some movement in the hand, the object may reach the goal.

It is difficult for the object to enter the hand if the object is entirely free from any obstacles. Hence tests to evaluate *EoEn* are simulated under the same conditions as tests for *DoEs*. When we evaluate DoEs, the gate locates in the hand as the right figure of Fig. 7, and when we consider EoEn, the gate is outside of the closed region as the left figure of Fig. 7.

A. Indexes for Evaluation of Partial Caging

We evaluate difficulty of passing through the goal for the moving object with the following two indexes:

- *Index 1*: Average simulation time until the moving object reaches the goal,
- *Index 2*: Rate of cases that the moving object cannot reach the goal.

Thus higher score of the indexes indicates larger difficultly for the object to enter the hand or escape from the hand. The index 1 is also proposed in [5], and the index 2 is introduced in our scheme due to limitation of computing time.

After simulations, we obtain each index of both *EoEn* and *DoEs* under a particular conditions. And then we calculate a new index score,

$$\frac{Index\ of\ DoEs}{Index\ of\ EoEn}, \tag{12}$$

which represents that the form (or posture) of the hand is good both for capturing an object without any finger motions and for confining it geometrically.

B. Simulation Settings

Every length of the hand is as following: ($L_{11} = L_{21} = 500$ [mm]; $L_{12}, L_{13}, L_{21}, L_{22}, L_{23}$ is changed by the parameters of the goal gate: $L_g (= L_{13} = L_{23})$ and $W_g := \|\boldsymbol{p}_{13} - \boldsymbol{p}_{23}\|$; the length of the palm is $L_p = 500$ [mm]. Since the hand forms a rectangular shape, the joint variables, $|\theta_{11}| = |\theta_{12}| = |\theta_{21}| = |\theta_{22}| = \frac{\pi}{2}$. Then the length of the fingers is determined as $L_{12} = L_{22} = \frac{L_p - W_g}{2}$. The coefficient of restitution between the object and every limb, $e_r = 0.1$.

We solve the ordinary differential equations (4) and (11) with the 4th-order Runge-Kutta Method. The step size of the solver, $dt = 0.001$, that is, the discrete time is assumed to be 1 [ms]. The gravitational acceleration in the reference frame, $\boldsymbol{g}_O := [0, 0, -9.8]^T$ [m/s^2]. The limitation of simulation steps is 600,000, that is, the maximum elapsed time in the simulation is assumed to be 10 minutes.

The joint angles of the manipulator inclining the hand, θ_{j1}, θ_{j2} are changed every 10,000 steps (10 [s]). The range of each angle is respectively $-\pi/6 < \theta_{j1} < \pi/6$ and $-\pi/6 < \theta_{j2} < \pi/6$ [rad]. Each desired angle is randomly determined every 10,000 steps (10 [s]), and each angle changes to the desired value in uniform angular velocity in 1,000 steps (1 [s]). Thus each joint keeps the desired joint variable in other 9,000 steps (9 [s]).

Initial position of the moving point in each simulation is randomly selected near the foot of the fingers (that is, both ends of the palm). And every initial velocity is always 0 [m/s]. A random number generator of the GSL (GNU Scientific Library [15]) is used as the algorithm of *Mersenne Twister*.

When the simulation steps reach the limitation defined above, the limitation steps, 600,000 is used to calculate the average steps, *index 1*. Trials for each simulation setting are executed 5,000 times with a different seed of random number generator.

C. Simulation Results: for Evaluating Difficulty of Escaping

We evaluate the *index 1* and *index 2* defined above with changing the arrangement of finger: width of the goal, W_g, angle of the fingertip, θ_g, and the radius of the circular object, r_o. In Sec. III-C, we discuss on the difficulty of escaping from the hand and the effect by the arrangement of the fingertips.

1) Changing the Width of the Goal: In this analysis, we set the length of the gate (fingertip), $L_g = 0.2L_p$ [mm], the angle of the fingertip $\theta_g = 0, \pm 10$ [deg] each, and change the width of the goal, W_g, to $0.4L_p, 0.6L_p, 0.8L_p$ [mm] with setting the length of the limbs: $L_{12} = L_{22} = 0.3L_p, 0.2L_p, 0.1L_p$ respectively. And the radius of the object r_o is equal to $0.01L_p$.

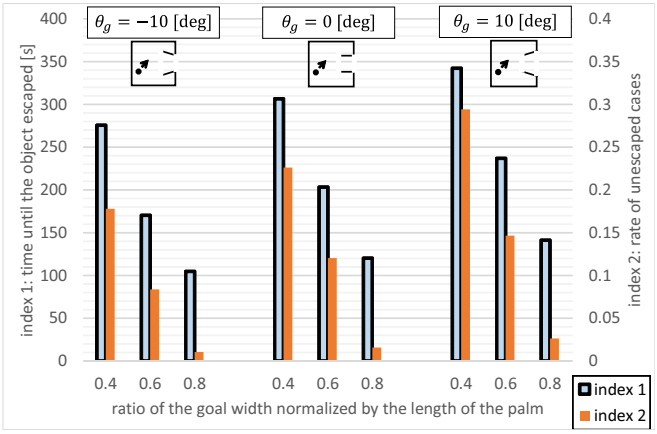

Fig. 8. Difference of difficulty of escaping from the hand related to the width of the gap between both fingertips (the goal)

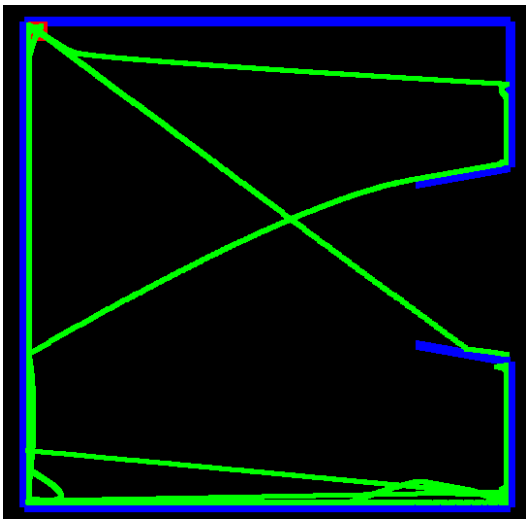

Fig. 9. An Example of locus of the moving point ($L_g = 0.2L_p$, $W_g = 0.4L_p$, $\theta_g = 10$ [deg]). Red: an initial position of the moving point; blue: limbs; green: locus of the moving point

The results of *index 1* and *index 2* with various width of the goal are shown in Fig. 8. It is intuitive that the difficulty of escaping for the object decreases according to increase of the width of the goal. Fig. 9 is an example of locus of the moving point.

2) Changing the Angle of the Gate: In this analysis, we set the width of the goal, $W_g = 0.4L_p, 0.6L_p, 0.8L_p$[mm], the length of the goal gate (fingertip) $L_g = 0.2L_p$[mm], and change the angle of the gate, θ_g. The radius of the object is $r_o = 0.01L_p$.

The results of the *index 1* and *index 2* related to angle of the gate in the case of $W_g = 0.4L_p$ are shown in Fig. 10(a), and a similar trend between both indexes can be seen. For instance, coefficient of correlation between the index 1 and index 2 in Fig. 10(a) is 0.984. Therefore only the results of index 1 are presented in later discussion. Fig. 10(b) shows changing of index 1 related to angle of the gate, with various

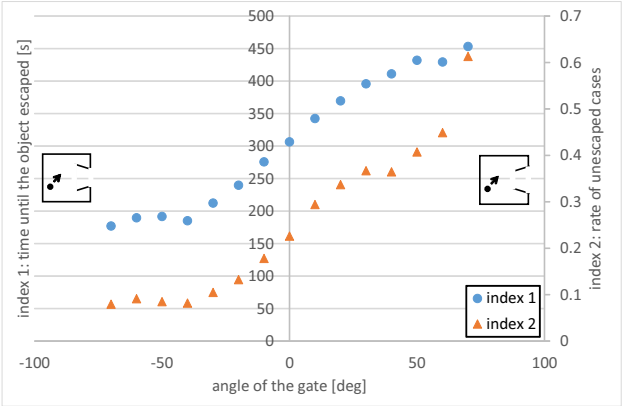

(a) Differences of index 1 and index 2 while $W_g = 0.4L_p$

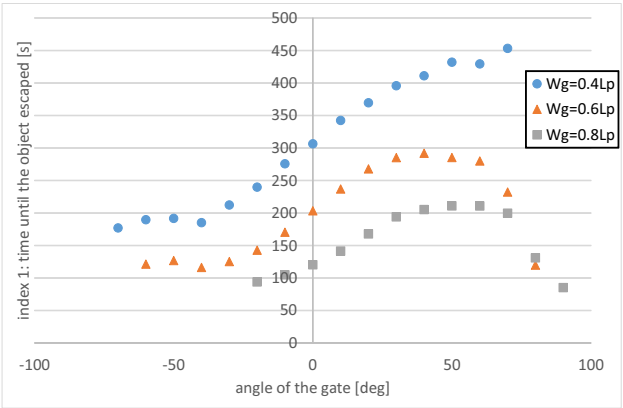

(b) Differences of index 1 while $W_g = 0.4L, 0.6L, 0.8L$

Fig. 10. Difference of difficulty of escaping from the hand related to angle of the fingertips (the gate)

width of the gate.

Let us see Fig. 10 while $W_g = 0.4L_p$. The index score, which expresses the difficulty of escaping for the object, almost increases according to θ_g. excepting slight decrease of index 2 about $\theta_g = 40$ [deg] (Fig. 10(a)).

When we set the width of the gate larger: $W_g = 0.6L_p, 0.8L_p$, *index 1* increase while $\theta_g \leq 40, 50$ [deg], and they decrease after the peak, respectively. (Fig. 10(b) while $W_g = 0.6L_p, 0.8L_p$).

The range of angle of the gate is changed for each W_g because the minimum width of gap between fingertips or finger limbs, where the object cannot pass through, are built by large angle. For example, the object cannot reach the corner around finger joints, $\boldsymbol{p}_{12}, \boldsymbol{p}_{22}$ when $W_g = 0.6L_p, \theta_g = -70$ [deg] because of located fingertips. And then the object can easily head to the goal traveling along the fingertip.

D. Discussion on Difficulty of Escaping

From the results in Sec. III-C.1, the difficulty of escaping from the semi-closed hand for the circular object is assumed to decreases according to the width of the gate. Thus the difficulty almost increases according to angle of the gate, θ_g increases, excepting slight decrease of index 2 about $\theta_g = 40$ [deg] while $W_g = 0.4L_p$. On the other hand, the

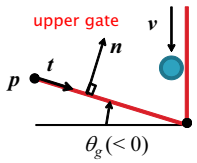

Fig. 11. In a case that the circular object moves along the limb and dive into the wedge-shaped space at the fingertip

index scores in the cases with $W_g = 0.6L_p, 0.8L_p$ have each peak and decrease at more than the angle. These results are assumed to be caused by the following two factors.

1) Retention of the Object and Getting Over the Gate: The one factor is the retention of the moving object around the foot of the gate when θ_g is small, particularly $\theta_g < 0$. Then the velocity of the object can be easily decreased.

Let us consider that the moving point moves along the vertical limb and dive into a wedge-shaped space at the fingertip. (Fig. 11). When the velocity of the moving point before rebound with the gate, $\boldsymbol{v}_0 = [0, -v]^T$, and the unit normal vector of the gate, $\boldsymbol{n} = [-\sin\theta_g, \cos\theta_g]^T$, the velocity of the moving point after rebound, $\boldsymbol{v}$ can be calculated as follows:

$$\boldsymbol{v} = \begin{bmatrix} -(1+e_r)v\sin\theta_g\cos\theta_g \\ v\left\{(1+e_r)\cos^2\theta_g - 1\right\} \end{bmatrix}. \tag{13}$$

Thus the moving object remains the wedge-shaped space when $\theta_g < 0$ [deg], and the speed of it after rebound depends on the absolute value of θ_g. Moreover the direction of the gravitational acceleration applied to the object to let it escape from the narrow space is limited. On the other hand, when θ_g is large, particularly $\theta_g > 0$ [deg], the velocity of the moving point after rebound with the gate such above case can change its direction and keep a certain amount of its speed. Therefore large θ_g can prevent the moving object from remaining around the foot of the gate.

We verify the above hypothesis by simulations examined as the following procedures.

Step 1. Set the moving object near the joint, $\boldsymbol{p}_{22}$ at velocity 0 [m/s].
Step 2. Fix each joint angle of the hand, θ_{j1}, θ_{j2} and the gate angle θ_g.
Step 3. Let the moving object in free movement. After that, the object goes along the limb and collides with the gate.
Step 4. Observe whether the object gets over the gate and goes into the goal.
Step 5. Iterate above steps with changing $\theta_{j1}, \theta_{j2}, \theta_g$.
Step 6. Calculate *index 2* for each case.

From (3) and the range of θ_{j1} and θ_{j2}, the conditions for the object to reach the goal are at least:

$$\begin{cases} g\sin\theta_{j1} > 0, \\ -g\cos\theta_{j1}\sin\theta_{j2} < 0, \end{cases} \tag{14}$$

$$\therefore 0 < \theta_{j1}, \theta_{j2} < \frac{\pi}{6}. \tag{15}$$

Thus we change each joint angle from 0 to 30 [deg] by 1 [deg], and test the above steps with all the combinations,

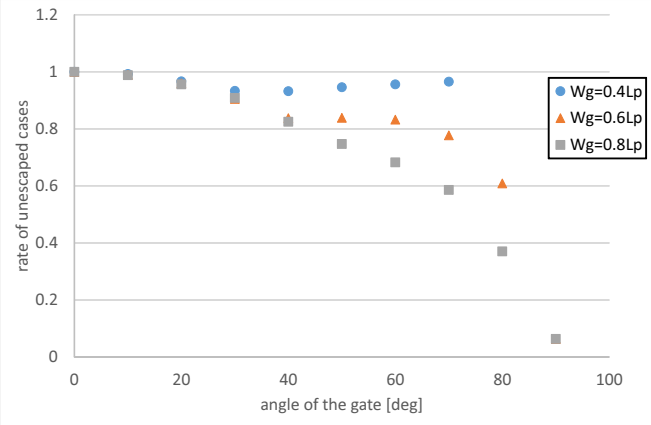

Fig. 12. Differences of the rate of unescaped cases from the hand related to angle of the fingertip (the gate)

961 patterns for each θ_g. In addition, we note that $\theta_g > 0$ is necessary for the object to escape because the object never get over the gate under the conditions of (15) while $\theta_g \leq 0$. Expected behaviors of the object are three patterns: remaining around foot of the gate; getting over the gate but jumping it over; or getting over the gate and going into the goal.

We set the gate parameters as $L_g = 0.2L_p$ [mm], $W_g = 0.4L_p, 0.6L_p, 0.8L_p$. Fig. 12 shows the results of the examination. In the cases of $W_g = 0.4L_p$, the rate of the cases that the object does not escape (index 2) is slightly decreased when the angle of the gate, θ_g, is about 40 [deg]. The tendency of the result is similar to that of Fig. 10(a). It is because larger angle of the gate facilitates the object getting over the gate. However the larger angle makes the width of the gate narrower. Hence the object can easily jump over the gate, which can be seen $\theta_g > 50$ [deg] in the simulations.

On the other hand, when $W_g = 0.6L_p, 0.8L_p$, the width of the gate is enough wide for the object to reach the goal even when the angle of the gate, θ_g, becomes larger than 40 [deg]. The tendency of these results is also similar to that of Fig. 10(b) while $\theta_g \geq 50$ [deg].

2) Width of the Gate: The other factor is decrease of the entrance width of the gate according to θ_g. From the reason mentioned above, θ_g is expected to be large to avoid retention of the moving point. However, the entrance width, which is calculated as $\left(W_g - 2L_g \sin\theta_g\right)$ decreases at that time, and the difficulty of escaping for the moving point increases.

Consequently, the value of θ_g affects the tendency of retention of the moving point and the entrance width of the gate, and both are trade-off for the difficulty of escaping from the hand for the object. When the width of the gate is enough wide for the object to escape such as $W_g = 0.6L_p, 0.8L_p$, an effect given by larger angle of the gate to avoid retention of the moving point is welcomed.

E. Simulation Results: for Evaluating Both Ease of Entering and Difficulty of Escaping

In the above analysis, we focused on difficulty of escaping (DoEs) from the hand for a circular object, and then every fingertip, which plays a role as a gate, locates inside the hand. Additionally in Sec. III-E, ease of entering the hand (EoEn) for an object outside the hand illustrated as the right figure of Fig. 7 is also evaluated by simulations. Moreover, we also address an ability of the hand in the point of geometrical capturing for objects, using the index derived in (12).

1) Changing the Radius of the Object: In this analysis, we fix the width of the goal, $W_g = 0.4L_p$[mm] and the length of the goal gate (fingertip) $L_g = 0.2L_p$[mm], and change the angle of the gate, θ_g for various size of the object: $r_o = 0.01L_p, 0.05L_p, 0.1L_p$.

According to the above two simulation results, *index 1* is correlated strongly with *index 2*. Thus in the analysis, similarly only the result of index 1 is presented (Fig. 13, 14).

From the result (Fig. 13), when the angle of the fingertips, $\theta_g \leq 10$ [deg], it has little interference in ease of entering for the object. It indicates that the object can easily reach the goal while $\theta_g \leq 0$ if only it enters the gap between the fingertips, whose width is $(W_g - 2L_g \sin\theta_g) \geq W_g$.

On the other hand, when $\theta_g \geq 0$, the width of the gap is $(W_g - 2L_g \sin\theta_g) \leq W_g$, and then, collisions between the object and the gates prevent the object from reaching the goal. Therefore narrower gap caused by larger gate angle, θ_g spends more time that elapses before the object reaches the goal, especially for small objects.

As concerns the difficulty of escaping from the hand related to angle of the gate (Fig. 14), all the cases have same trend as that the difficulty increases according to the gate angle θ_g, as mentioned in Sec. III-C.2.

2) Evaluating of Partial Caging: With (12), we define an index score of partial caging that evaluates whether the configuration of the hand is good both for capturing an object without any finger motions and for confining it geometrically. The index is calculated from two results: Fig. 13 and 14, and is shown in Fig. 15.

From the result, the index score is high about $\theta_g = 10$ [deg] regardless of the size of the object. Hence it means that a robot hand under this condition, $\theta_g = 10$ [deg], has an appropriate ability of both capturing an circular object easily and confining without any finger motion.

On the other hand, in cases that the radius of the object, r_o is small, the score decreases in inverse relation to θ_g. It is because that narrower gate prevents the object from not only escaping from the hand but also entering there.

IV. Conclusions and Future Works

In this paper, we investigated an evaluation of ability of a robot hand for capturing objects and confining it geometrically as partial caging. Considering a simplified scenario in which a planar two-fingered hand captures a circular object, we evaluate both ease of entering the hand and difficulty of escaping from there for the object. The difficulty of escaping mainly depends both on the width of the gap between fingertips, which is called as a goal, and on retention at the foot of the fingertips acting as a gate. The width of the gap is determined by the parameters of the

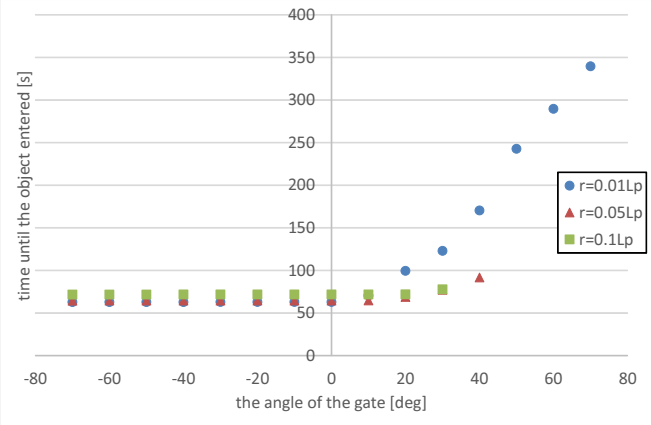

Fig. 13. Differences of difficulty of *entering the hand* related to angle of the fingertips

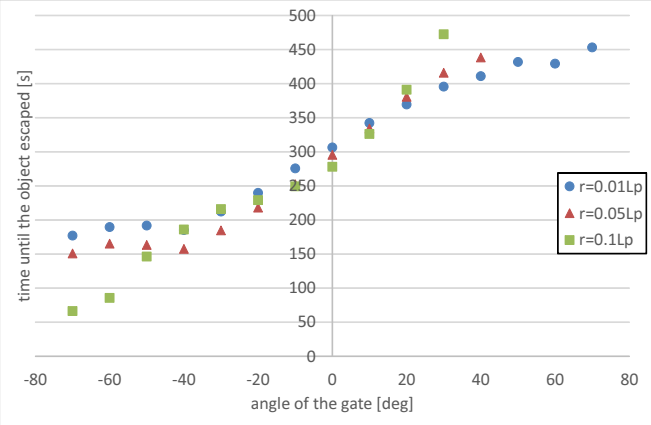

Fig. 14. Differences of difficulty of *escaping from the hand* related to angle of the fingertips

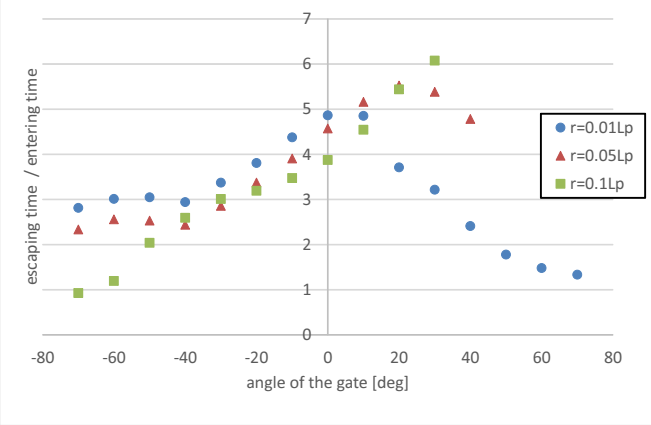

Fig. 15. Difference of index evaluating partial caging quality related to the angle of the fingertips

fingers: the length of limbs and the angle of joints. Widely opened gate with large joint angle typically facilitates the object escape through the gap. At that time, however, the large angle often causes retention of the object around the foot of the fingertip, and it makes the object difficult to escape. In regard to ease of entering the hand, angle of the fingertips hardly prevent the resultant object behavior, excepting closing gate angles for small objects.

In future works, more variety of hand configuration and objects such as sticks, boxes as general polygons, and curved shapes should be investigated. Moreover, partial caging in three dimensional scenes by a multifingered hand can be considered.

References

[1] E. Rimon and A. Blake, "Caging planar bodies by one-parameter two-fingered gripping systems," *Int. J. of Robotics Research*, vol. 18, no. 3, pp. 299–318, March 1999.

[2] P. Pipattanasomporn and A. Sudsang, "Two-finger caging of nonconvex polytopes," *IEEE Trans. on Robotics*, vol. 27, no. 2, pp. 324–333, April 2011.

[3] R. Diankov, S. S. Srinivasa, D. Ferguson, and J. Kuffner, "Manipulation planning with caging grasps," in *Proc. of IEEE/RAS Int. Conf. on Humanoid Robots*, Daejeon, Korea, December 2008, pp. 285–292.

[4] S. Makita and Y. Maeda, "3D multifingered caging: Basic formulation and planning," in *Proc. of IEEE/RSJ Int. Conf. on Intelligent Robots and System*, Nice, France, October 2008, pp. 2697–2702.

[5] T. Makapunyo, T. Phoka, P. Pipattanasomporn, N. Niparnan, and A. Sudsang, "Measurement Framework of Partial Cage Quality," in *Proc. of IEEE Int. Conf. on Robotics and Biomimetics*, Guangzhou, China, December 2012, pp. 1812–1816.

[6] W. Kuperberg, "Problems on polytopes and convex sets," in *DIMACS Workshop on Polytopes*, January 1990, pp. 584–589.

[7] A. Rodriguez and M. T. Mason, "Two finger caging: Squeezing and stretching," in *Proc. of Int. Workshop on the Algorithmic Foundation of Robotics*, Guanajuato, México, 2008.

[8] M. Vahedi and A. F. van der Stappen, "Caging polygons with two and three fingers," *Int. J. of Robotics Research*, vol. 27, no. 11-12, pp. 1308–1324, November/December 2008.

[9] J. Erickson, S. Thite, F. Rothganger, and J. Ponce, "Capturing a convex object with three discs," *IEEE Trans. on Robotics*, vol. 23, no. 6, pp. 1133–1140, December 2007.

[10] G. A. S. Pereira, M. F. M. Campos, and V. Kumar, "Decentralized algorithm for multi-robot manipulation via caging," *Int. J. of Robotics Research*, vol. 23, no. 7-8, pp. 783–795, July/August 2004.

[11] Z. Wang and V. Kumar, "Object closure and manipulation by multiple cooperating mobile robots," in *Proc. of IEEE Int. Conf. on Robotics and Automation*, Washington D.C., U.S.A., May 2002, pp. 394–399.

[12] Y. Maeda, N. Kodera, and T. Egawa, "Caging-based grasping by a robot hand with rigid and soft parts," in *Proc. of IEEE Int. Conf. on Robotics and Automation*, St. Paul, USA, May 2012, pp. 5150–5155.

[13] W. Wan, R. Fukui, M. Shimosaka, T. Sato, and Y. Kuniyoshi, "Grasping by caging: A promising tool to deal with uncertainty," in *Proc. of IEEE Int. Conf. on Robotics and Automation*, St. Paul, MN, USA, May 2012, pp. 5142–5149.

[14] Y. Jiang, C. Zheng, M. Lim, and A. Saxena, "Learning to place new objects," in *Proc. of IEEE Int. Conf. on Robotics and Automation*, St. Paul, MN, USA, May 2012, pp. 3088–3095.

[15] Free Software Foundation, Inc., "GSL (GNU Scientific Library)," http://www.gnu.org/software/gsl/.